ELSEVIER

Journal of Fluids and Structures 25 (2009) 1272–1281

JOURNAL OF FLUIDS AND STRUCTURES

www.elsevier.com/locate/jfs

By-pass transition to airfoil flutter by transient growth due to gust impulse

M. Schwartz, S. Manzoor, P. Hémon*, E. de Langre

LadHyX, CNRS-Ecole Polytechnique, F-91128 Palaiseau, France

Received 16 May 2008; accepted 13 August 2009
Available online 30 October 2009

Abstract

We present an experimental study which shows that the mechanism known as transient growth of energy, can cause flutter instability of a nonlinearly flexible airfoil at a wind velocity below the linear critical flutter velocity. A flap mounted upstream a flexible airfoil in a wind tunnel generates a single gust which triggers the plunge and pitch oscillations. This gust is characterized using two-component hot-wire anemometry. For the first time experimental evidence is provided to confirm the theoretical scenario of a by-pass transition to flutter by transient growth. From an engineering point of view, transient growth might explain also the premature structural fatigue encountered in structures subject to wind.

Keywords: Flutter; Transient growth; By-pass transition; Aeroelasticity

1. Introduction

In linear flutter studies, it is common to assume that the long-term system amplitude behaves exponentially in time, decaying or growing depending on the mean wind velocity $\bar{U}$. The analysis then follows a normal modes approach where the long time behaviour is sought, in terms of the critical value of the wind velocity U_c which determines the limit between stable and unstable cases. As presented in Fig. 1(a), an initial perturbation is damped at a velocity below the critical velocity or amplified at a velocity larger than U_c.

However, it has been shown by Schmid and de Langre (2003) that it is possible to observe a transient increase of energy at a velocity below U_c. In a linear case this mechanism leads initially to an amplification of the energy of the system that subsequently decreases due to stable conditions. This is called transient growth of energy. It is a consequence of non-orthogonal modes involved in the system (Schmid and Henningson, 2001). Transient growth is a linear mechanism by nature and applies to linear or nonlinear systems. It depends strongly on the initial conditions produced by the initial perturbation. An experimental evidence of transient growth, illustrated by behaviour of type A in Fig. 1(a), was given by Hémon et al. (2006) for a linearly flexible airfoil in a wind tunnel.

In a nonlinear case, i.e. when the airfoil support elasticity behaves nonlinearly, the amplitude of the perturbation is an important parameter due to the subcritical branch as illustrated in Fig. 1(b), when the mean velocity is larger than the velocity U_{cnl} and below the linear critical velocity U_c. An initial small perturbation keeps the system in the stable region

*Corresponding author. Tel.: +33 1 69 33 52 76; fax: +33 1 69 33 52 92.
E-mail address: pascal.hemon@ladhyx.polytechnique.fr (P. Hémon).

0889-9746/$ - see front matter © 2009 Elsevier Ltd. All rights reserved.
doi:10.1016/j.jfluidstructs.2009.08.001

Nomenclature

M_O	aerodynamic momentum about O (N m)
b, c	span and chord of the profile (m)
d	distance between gravity centre and O (m)
$E(t)$	total mechanical energy (J)
E_0	initial mechanical energy (J)
$E_{\max}$	maximum of the mechanical energy (J)
F_z	lift force (N)
f_α , f_z	frequencies of pure motions (Hz)
f_1, f_2	frequencies of the coupled motion (Hz)
J_O	inertia about O (kg m^2)
k_α, k_z	stiffness (N m/rad) and (N m^{-1})
m	mass involved in the vertical motion (kg)
$\bar{U}$	mean wind velocity (m s^{-1})
U_r	reduced velocity ($U_r = \bar{U}/c f_z$)
$z(t)$	plunge (m)
g	gap for nonlinear case (m)
$\alpha(t)$	pitch angle about O (rad)
δk	nonlinear flexion stiffness (N m^{-1})
η_α, η_z	reduced structural damping (%)
λ_α, λ_z	eigenvalues of pure motions (rad^2 s^{-2})
λ_1, λ_2	eigenvalues of coupled motions (rad^2 s^{-2})
ω_α, ω_z	angular frequencies of pure motions (rad s^{-1})

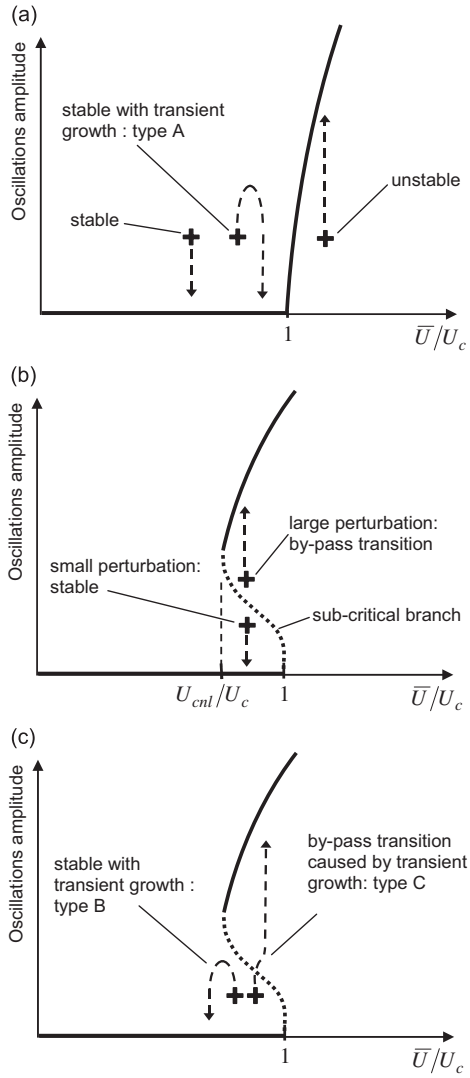

Fig. 1. (a) Effects of an initial perturbation for a linear system, (b) perturbation amplitude effect for a nonlinear system and (c) scenario of by-pass transition due to transient growth of an initial perturbation.

but for a larger initial perturbation, the system state may reach the unstable region, leading to flutter even below U_c. This scenario is called by-pass transition to flutter by amplitude effect.

But there is another possible scenario in which an initial small perturbation can be amplified linearly by transient growth because the mean velocity is just below the linear critical velocity. As illustrated in Fig. 1(c), two possibilities can exist

(i) the transient amplification remains small and keeps the system stable (referred to as type B in Fig. 1(c));
(ii) the transient amplification is such that the system response then reaches the subcritical branch, and flutter instability is triggered (referred to as type C).

The latter is also a by-pass transition to flutter, but caused by transient growth of a small initial perturbation, the level of which would have led to stability without this amplification. It is therefore different from a classic by-pass transition where the initial amplitude alone triggers the flutter instability. A similar mechanism is a possible scenario in the domain of transition to turbulence (Schmid and Henningson, 2001).

The objective of this paper is to present an experimental study that confirms the existence of this theoretical scenario of by-pass transition caused by transient growth. Significant differences with the previous experimental study of transient growth (Hémon et al., 2006) are (i) a nonlinear device is now added to the elastic support of the airfoil, (ii) the initial perturbation is generated now by an upstream flap, instead of a mechanical excitation of the airfoil. This produces a set of initial conditions on the dynamical system which is controlled by the unsteady aerodynamic response of the airfoil to the upstream velocity perturbation. This way of excitation renders the study more realistic and pertinent for practical applications.

Other previous experimental studies have already dealt with nonlinear airfoil flutter, for instance by Marsden and Price (2005), but none of them have analysed the transient behaviour of such a system. Numerically, Lee et al. (2005) have focused their investigation on the mechanisms leading to limit cycle oscillations. They mainly investigated the supercritical velocity range although they mention ''strong energy exchange between modes'' at subcritical velocities, which might be the consequence of transient growth of energy. More recently the transient growth in sliding friction systems has been numerically studied by Hoffmann (2006). The by-pass transition caused by transient growth was found to be responsible for limit cycle existence in linearly stable conditions. However, an experimental study that could confirm this mechanism has never been presented yet.

In this paper, we present first the experimental aeroelastic setup, the identification of the gust impulse which is used for generating the initial perturbation and the nonlinear airfoil parameters. Then the results are presented in order to confirm the existence of a by-pass transition to flutter due to transient growth.

2. Experimental techniques

2.1. Experimental set-up

A NACA 0015 profile made of plexiglas is mounted in the test section of a small Eiffel wind tunnel at LadHyX (see Figs. 2 and 3). It is an improvement of the set-up which was previously used by some of the authors (Hémon et al., 2006). The square test-section is 180 mm wide. The profile is allowed to oscillate in plunge and pitch. The airfoil has a chord $c = 0.12$ m and a span width $b = 0.17$ m. The rotation centre O is located at the forward quarter chord and the gravity centre G is at the distance d behind O. The mean angle of attack is set to zero. Sand grains are glued near the leading edge in order to trigger the boundary layer laminar–turbulent transition always at the same place during the experiments. Two end plates are mounted at the extremities in order to further a 2-D flow.

Dynamics of the system is set by means of linear springs for plunge and pitch, as sketched in Fig. 3. In this new set-up, special care has been taken to minimize the structural damping of the system: especially, no bearings are involved in the design, thus avoiding any friction between moving parts. The nonlinear feature is provided on the plunge degree of freedom by two linear contact springs which respond only if the amplitude is larger than a gap value. Two systems are used: one referred to as linear without contact springs, and a second one referred to as nonlinear with the contact springs mounted.

2.2. Measurement techniques

The reference mean wind velocity $\bar{U}$ is measured with a Pitot tube connected to an electronic manometer. A thermocouple measures the ambient temperature for correcting the reference wind velocity. Precision is of the order of

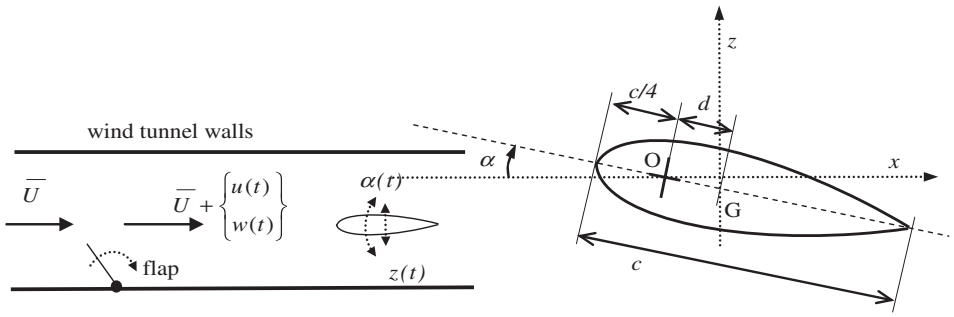

Fig. 2. Principle of the experiments and airfoil geometrical parameters.

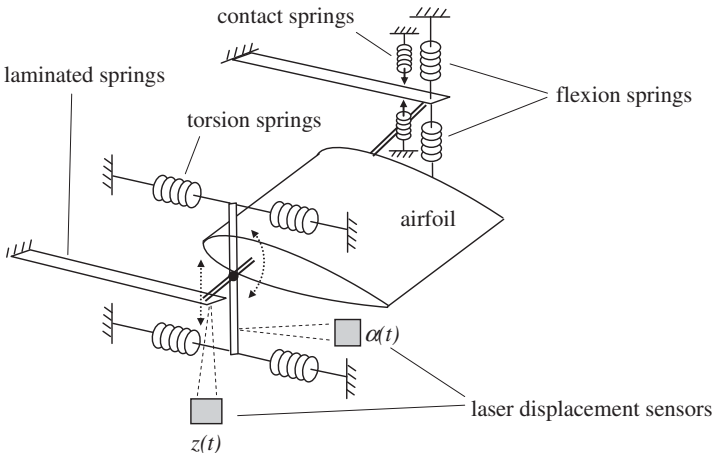

Fig. 3. Kinematics of the flexible airfoil.

0.2%. Typical Reynolds number of the experiments, based on the chord, is in the range 80 000–120 000. Turbulence level in the empty test-section is about 1%.

The two motions are measured with two laser displacement sensors connected to a high speed acquisition and signal processing device. The physical degrees of freedom z and α versus time are provided by recombination of the measured signals using the system kinematics. By using static calibration, the resulting precision is around 1%.

All these signals are connected to an acquisition system PAK provided by Mueller-BBM. It consists mainly of a 24-bit 8-channel acquisition card and signal processing software. Typical duration of acquisition is 10 s with a sampling frequency of 8192 Hz.

2.3. Perturbation identification

The initial perturbation is provided by a flap mounted on the wind tunnel floor upstream the profile, as presented Fig. 2. The dimensions of the flap are 45 mm length and 170 mm width. The rotation axis of the flap is located 160 mm upstream the wing rotation axis. By using a tensioned spring which is suddenly released, the flap generates a short impulse $u(t)$, $w(t)$ which adds to the upstream wind velocity $\bar{U}$. The characteristics of this perturbation have been measured with two components hot wire anemometry. The global precision is of 5%, and regular calibrations were performed during the test series in order to take into account the air temperature evolution.

The flap generates a transient short impulse on the wind velocity, leading to a unique peak in the longitudinal component u, and simultaneously two peaks in the vertical component w, one negative and one positive. An example of time histories of $u(t)$, $w(t)$ is shown in Fig. 4. Time duration of this perturbation is about 0.05 s, which is three times

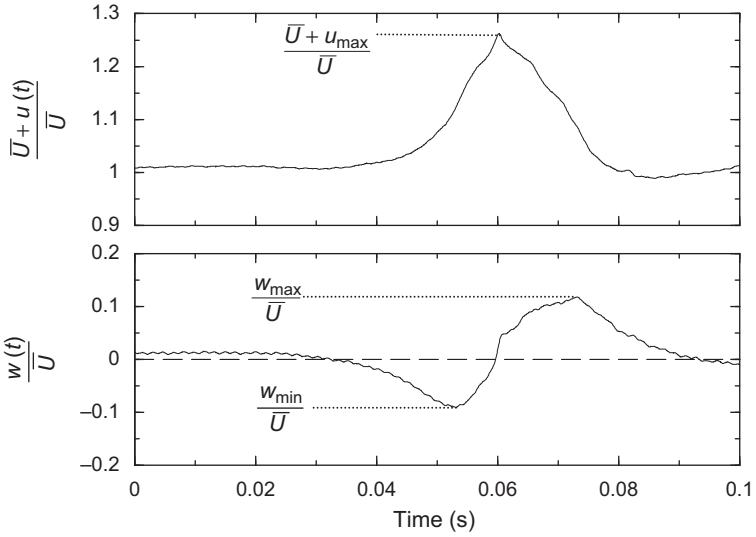

Fig. 4. Measured sample of upstream velocity perturbation.

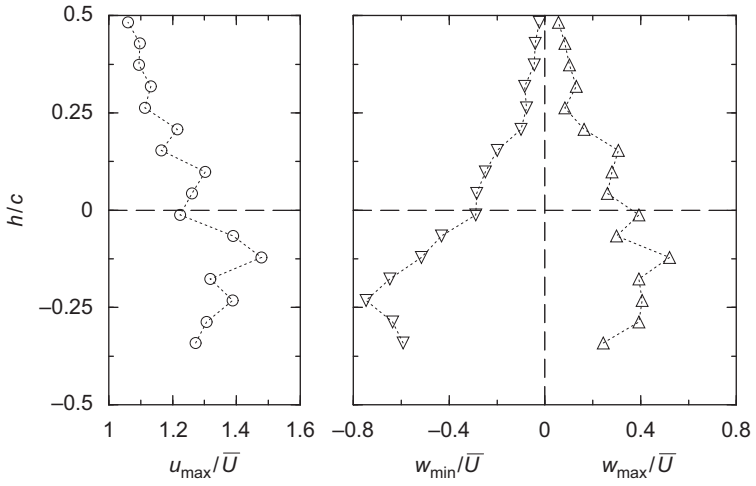

Fig. 5. Characteristics of the instantaneous upstream velocity perturbation along vertical axis of the test-section at the leading edge longitudinal position ($\bar{U} = 10\,\mathrm{m/s}$).

below the typical period of the two airfoil degrees of freedom. An initial instant reference is deduced by using the signal from an accelerometer mounted on the flap. It is also used to trigger the measurements. The time for the disturbance to reach the airfoil was estimated by comparing accelerometer and hot wire signals. It is 0.08 s for $\bar{U} = 17\,\mathrm{m/s}$ and decreases by increasing wind tunnel velocity.

These characteristic parameters have been measured in the empty test-section along the vertical axis of the section, at the longitudinal position of the airfoil leading-edge. Results of instantaneous flow quantities are plotted in Fig. 5 versus the height of the section reduced by the chord of the profile. Position zero corresponds to the middle of the section, where the airfoil leading-edge normally stands.

The influence of the mean velocity has been investigated also and reported in Fig. 6. Varying the undisturbed flow velocity in the experiments, a small influence is found on the longitudinal component u, with a small positive slope, while the vertical component w remains almost constant.

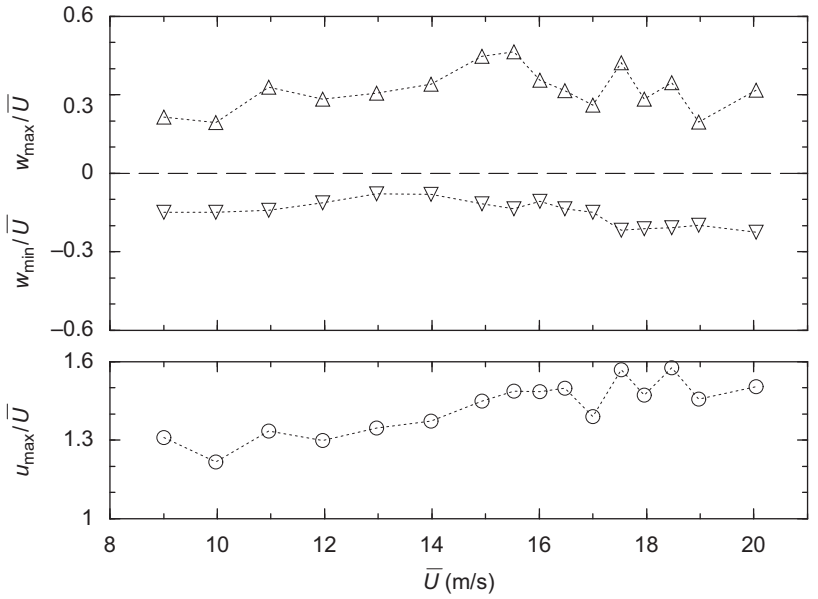

Fig. 6. Characteristics of the instantaneous upstream velocity perturbation versus mean velocity at the leading edge position.

2.4. Identification of structural parameters without nonlinearities

The procedure is similar of that in Hémon et al. (2006) and is briefly recalled here. The equations of motion for plunge $z(t)$ and pitch $\alpha(t)$, read (Fung, 1993)

$$\begin{aligned} &m\ddot{z} + 2m\eta_z\omega_z\dot{z} + k_z z + md\ddot{\alpha} = F_z,\\ &J_O\ddot{\alpha} + 2J_O\eta_\alpha\omega_\alpha\dot{\alpha} + k_\alpha\alpha + md\ddot{z} = M_O. \end{aligned} \tag{1}$$

By assuming that the structural dampings are small, the eigenvalues for the non-coupled case ($d = 0$) are

$$\lambda_\alpha = \omega_\alpha^2 = \left(2\pi f_\alpha\right)^2 = k_\alpha/J_O, \quad \lambda_z = \omega_z^2 = \left(2\pi f_z\right)^2 = k_z/m. \tag{2}$$

For the more general coupled case, it can be shown that the distance d between the centre of gravity and the axis of rotation modifies the eigenvalues so that

$$\lambda_1 + \lambda_2 = (\lambda_z + \lambda_\alpha)\frac{1}{1 - md^2/J_O}, \tag{3}$$

where the eigenvalues of the coupled system are λ_1 and λ_2. The structural parameters are determined without wind. First we deal with the two motions separately. We measure the natural frequencies f_α and f_z by spectral analysis and the stiffness k_α and k_z by static calibration. Then we deduce the inertia J_O and m from Eq. (2). Pure structural dampings η_z and η_α are also determined using a standard decrement technique. They have been found to be very small, respectively, 0.2% and 0.15% of the critical damping, as this set-up was specifically designed with this objective. This result confirms the assumption leading to Eq. (2) where the effect of damping was neglected. The frequencies f_1 and f_2 of the coupled system are then measured and the distance d is deduced from Eq. (3).

The linear aerodynamic loads can be modelled using flutter derivatives (Scanlan and Tomko, 1971)

$$\begin{aligned} &F_z = \tfrac{1}{2}\rho bc\bar{U}^2(H_1\dot{z} + H_2\dot{\alpha} + H_3\alpha + H_4 z),\\ &M_O = \tfrac{1}{2}\rho bc^2\bar{U}^2(A_1\dot{z} + A_2\dot{\alpha} + A_3\alpha + A_4 z), \end{aligned} \tag{4}$$

where the flutter derivatives, or aeroelastic coefficients, can be expressed with the help of an unsteady airfoil theory (Fung, 1993). Here we calculate the pure aerodynamic damping terms H_1 and A_2, making the quasi-steady assumption (QST) (Hémon, 2006), so as

$$H_1 = \frac{-1}{\bar{U}}C_z', \quad A_2 = \frac{-1}{8}\frac{c}{\bar{U}}C_z'. \tag{5}$$

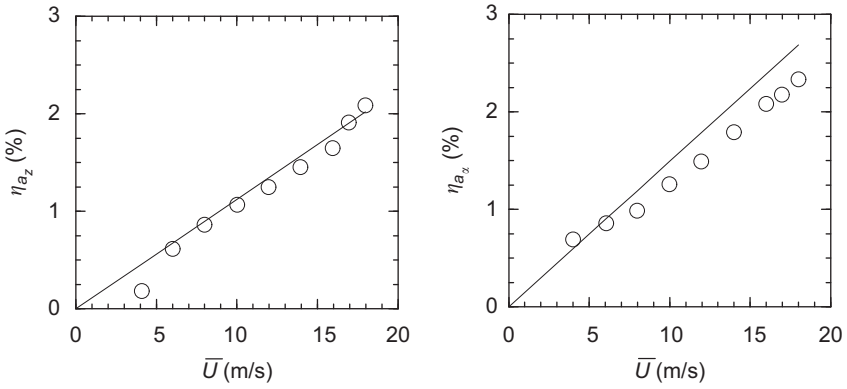

Fig. 7. Aerodynamic damping versus velocity: ○, experiment; —, QST.

Table 1
Values of system parameters.

k_α (N m/rad), k_z (N/m)	1.66 ± 0.05		881 ± 33
g (mm)		0.655 ± 0.04	
δk (N/m)		120 ± 5	
b, c (m)	0.12 ± 0.0001		0.17 ± 0.0001
f_α, f_z (Hz)	6.9375 ± 0.0625		4.9375 ± 0.0625
f_1, f_2 (Hz)	4.9375 ± 0.0625		7.4375 ± 0.0625
η_α, η_z (%)	0.2 ± 0.01		0.15 ± 0.01
J_0 (kg m^2), m (kg) from Eq. (2)	$8.74\ 10^{-4} \pm 0.25\ 10^{-4}$		0.915 ± 0.05
d (mm) from Eq. (3)		9.3 ± 0.3	

These aerodynamic damping terms are rewritten so as to be compared with reduced structural damping, which leads to

$$\eta_{a_z} = \frac{\rho b c \bar{U}}{4 m \omega_z} C'_z, \quad \eta_{a_\alpha} = \frac{\rho b c^3 \bar{U}}{32 J_O \omega_\alpha} C'_z. \tag{6}$$

Comparison with experimental values, using the lift derivative $C'_z = 2\pi$, is given in Fig. 7 for plunge and pitch. Good agreement is obtained which validates the experimental set-up and the structural parameters identification procedure.

The total energy is the sum of kinetic and potential energy which reads:

$$E(t) = \tfrac{1}{2} m \dot{z}^2(t) + \tfrac{1}{2} J_O \dot{\alpha}^2(t) + m d \dot{\alpha}(t) \dot{z}(t) + \tfrac{1}{2} k_z z^2(t) + \tfrac{1}{2} k_\alpha \alpha^2(t). \tag{7}$$

This quantity will be used to quantify transient growth. It will be nondimensionlized by the initial energy E_0 determined from the initial conditions. The maximum value of $E(t)$, as observed from the time series, will be denoted $E_{\max}$. All the measured and calculated parameters of the flexible system are given in Table 1.

2.5. Identification of parameters of the nonlinear system

The nonlinearity is located on the stiffness of the flexion due to the contact springs. Two parameters are needed, the gap g between the position zero and the contact, and the resulting stiffness $k_{nl} = k_z + \delta k$ above this gap. In fact the nonlinear system can be seen as a bilinear system, and the contact spring stiffness was chosen small enough so that the nonlinearity is relatively small.

The calibration is performed statically. This leads to a gap value $g = 0.655$ mm and an additional stiffness $\delta k = 0.136 kz$. The nonlinear feature of the flexural stiffness leads to an additional term on the energy that reads

$$E_{nl}(t) = \frac{\delta k}{4} \left\{ [|z - g| + (z - g)]^2 + [|z + g| - (z + g)]^2 \right\}. \tag{8}$$

This quantity is added to the energy (7) when measurements are performed with the nonlinear system.

3. Results

The experimental results are mainly presented by comparing the behaviour of the linear system, type A, and behaviours of the nonlinear system, type B or C, recalling that

(i) "A" corresponds to a transient growth of energy for a linear system, below the critical velocity U_c, and therefore is a stable case;
(ii) "B" is a transient growth of energy for the nonlinearly flexible airfoil, below the critical velocity U_c and stable;
(iii) "C" is identical to B except that the transient amplification of energy generates a by-pass transition to flutter instability.

The first measured quantities are the periods of the system, and their evolution versus the wind velocity is presented in Fig. 8 in terms of frequencies. The linear critical velocity U_c has been previously estimated by experiment. In the nonlinear system, the period depends on the amplitude of the motion. For the period measurements, plunge amplitude was then initiated manually during the recording so that the contact springs were always engaged. Since the gap g is small, the amplitude necessary to reach contact remains small, of the order of 1 mm. As the system is in fact weakly nonlinear, the resulting period can be considered as a mean value between a linear system having a stiffness k_z and another linear system having a stiffness $k_{nl} = k_z + \delta k$, with less than 14% between them. This effect can be observed at $\bar{U} = 0$ were the nonlinear system plunge frequency is just above that of the linear system (5.0625 Hz against 4.9375 Hz).

In the linear system at the onset of flutter the two frequencies coalesce. In the nonlinear case, the coalescence of the two frequencies occurs at a velocity U_{cnl} which is lower than in linear case. For a velocity above U_{cnl} and below U_c, a by-pass transition to flutter is therefore possible.

The transient growth of energy is now measured. The test procedure is as follows: (a) the flap is set in position with its torsion spring, (b) the wind tunnel velocity is adjusted to the desired value, (c) the flap is released manually and the accelerometer, which is mounted on it, triggers automatically the measurements, (d) after recording, the time history of total energy of the system is computed and plotted and (e) the initial value E_0 and the maximum $E_{\max}$ are read.

All data is collected and finally presented in Fig. 9, for the linear case, type A, and the nonlinear cases, types B and C. The region covered by the unstable behaviour of type C is shown hatched. When the system is unstable, the motion amplitude grows rapidly and it is stopped manually as the set-up is not designed for high amplitude limit cycle oscillations.

Just below critical velocity with the linear system, the type A presents an amplification level that is 9 times the value of initial energy. With the nonlinear system, the behaviour follows the evolution of the linear system for low velocities. Then, approaching the value U_{cnl}, the energy growth rate is higher than in linear case, and finally transition to flutter occurs, after an amplification larger than 7.

The comparison between linear and nonlinear behaviour is essential for the confirmation of the by-pass transition due to transient growth, because this is not a simple by-pass transition by initial amplitude effect. We must show indeed

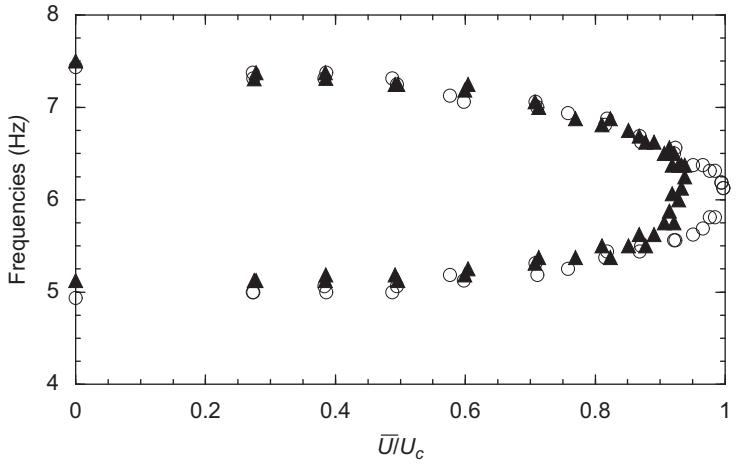

Fig. 8. Frequencies of the two modes versus velocity parameter: ○, linear case; ▲, nonlinear case.

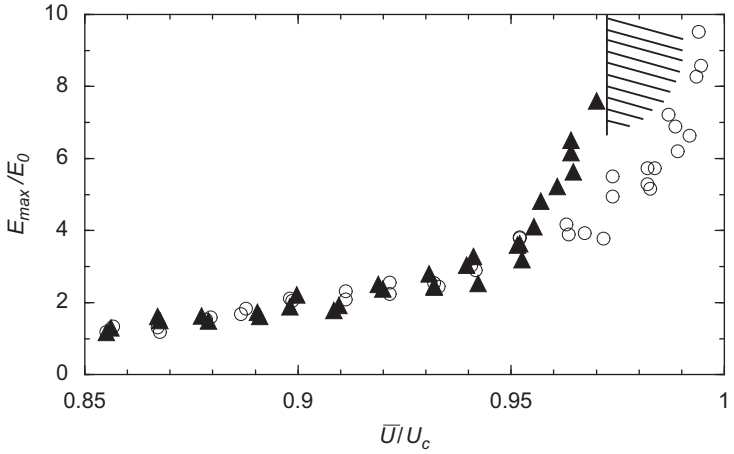

Fig. 9. Amplification rate of energy versus velocity parameter: ○, linear, type A; ▲, nonlinear, type B; and ▨, nonlinear, type C with by-pass transition caused by transient growth.

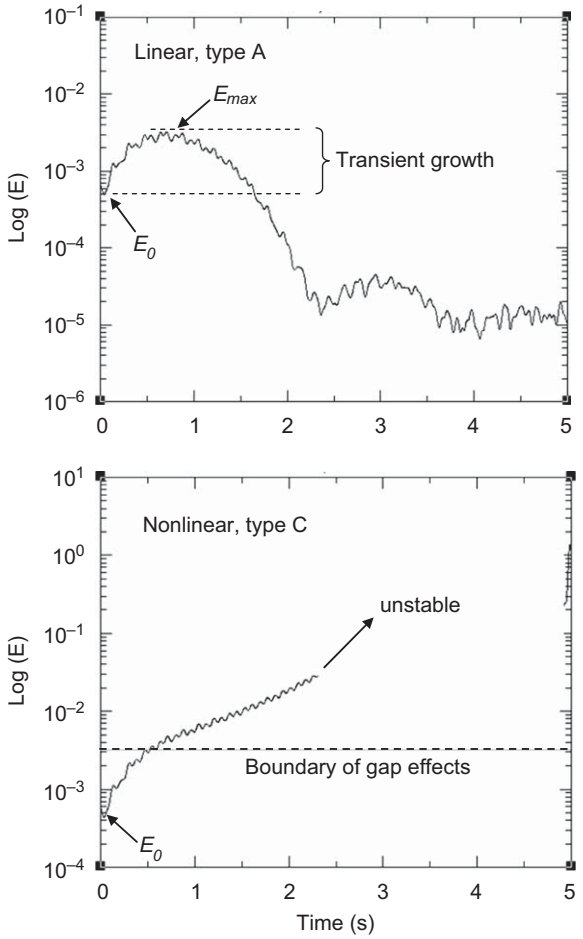

Fig. 10. Energy time histories in linear and nonlinear cases at $\bar{U}/U_c = 0.99$.

that the initial perturbation produced by the flap generates a value of the energy which remains below the level of the energy for which the nonlinear behaviour occurs, i.e. that the plunge z remains below the value of g at the initial instant.

This is shown in Fig. 10 where we present time histories of the total energy in a linear case of type A and a nonlinear unstable case of type C. Wind velocity is just below the linear critical velocity: the system is stable for the linear case, and by-pass transition to flutter occurs for the nonlinear case. Before the perturbation is introduced, the background energy level is of the order 10^{-5} J, a level where the linear system returns to stable conditions. The initial perturbation of level E_0 is amplified by transient growth up to E_{max} for the linear case, while it triggers flutter in nonlinear case.

In the latter, the boundary of the nonlinear behaviour was determined statically. This energy level corresponds to the potential energy of the system when the displacement $z(t)$ reaches the value of g. Beyond this gap, the contact springs are engaged and contribute to the stiffness of the airfoil and the system behaves nonlinearly.

Fig. 10 shows that the initial energy generated by the flap is well below the nonlinear boundary, and that the transient growth is in fact responsible for transition to flutter. For the first time, a by-pass transition generated by transient growth is observed experimentally in the domain of flow-induced vibrations.

4. Conclusion

Transient growth of energy is a linear mechanism in which a mechanical system submitted to a flow can display transient amplification of an initial perturbation, even below the linear critical velocity (Schmid and de Langre, 2003; Hémon et al., 2006). This behaviour depends on initial conditions. Under the critical velocity and when the mechanical system is linear, it always returns to stable state.

But with a nonlinear system and the flow velocity close to the subcritical branch, it is possible theoretically that the initial perturbation is linearly amplified by transient growth to a level which triggers a by-pass transition to unstable state. In this paper we have shown it experimentally.

The demonstration has been made with an airfoil which is able to oscillate in plunge and pitch in a wind tunnel. A weak nonlinearity is located in the stiffness of the plunge motion. The initial perturbation is given by a flap mounted upstream of the test-section which generates a velocity disturbance. It transmits to the airfoil an initial energy which is subject to transient growth. By crossing the boundary of nonlinearity, this transient amplification of energy makes the system unstable in the nonlinear case, while energy reaches a maximum peak and further decreases in the linear case.

This mechanism is therefore different from the classical by-pass transition for which the initial perturbation level of energy must be beyond the nonlinear threshold in order to trigger flutter.

Acknowledgement

This research work was supported by AIRBUS France under the programme Wing Flutter (WINFLU).

References

Fung, Y.C., 1993. An Introduction to the Theory of Aeroelasticity. Dover, New York.

Hémon, P., de Langre, E., Schmid, P., 2006. Experimental evidence of transient growth of energy before airfoil flutter. Journal of Fluids and Structures 22, 391–400.

Hémon, P., 2006. Vibrations des structures couplées avec le vent. Editions de l'Ecole Polytechnique.

Hoffmann, N., 2006. Transient growth and stick–slip in sliding friction. Journal of Applied Mechanics 73, 642–647.

Lee, Y.S., Vakakis, A.F., Bergman, L.A., McFarkland, D.M., Kerschen, G., 2005. Triggering mechanisms of limit cycle oscillations due to aeroelastic instability. Journal of Fluids and Structures 21, 485–529.

Marsden, C.C., Price, S.J., 2005. The aeroelastic response of a wing section with a structural freeplay nonlinearity: an experimental investigation. Journal of Fluids and Structures 21, 257–276.

Scanlan, R.H., Tomko, J.J., 1971. Airfoil and bridge deck flutter derivatives. ASCE Journal of the Engineering Mechanics Division, 1717–1737.

Schmid, P., de Langre, E., 2003. Transient growth before coupled-mode flutter. Journal of Applied Mechanics 70, 894–901.

Schmid, P., Henningson, D.S., 2001. Stability and Transition in Shear Flows. Springer, New York.